

Photocatalytic oxidation of dichloroacetic acid and dichloroacetyl chloride on TiO_2 : active sites, effect of H_2O , and reaction pathways

Adrienne C. Lukaski and Darrin S. Muggli*

Department of Chemical Engineering, University of North Dakota, Grand Forks, North Dakota 58202-7107, US

Received 10 February 2003; accepted 8 May 2003

Photocatalytic oxidation (PCO) quickly oxidizes dichloroacetyl chloride and dichloroacetic acid to phosgene (COCl_2) and CO_2 on TiO_2 . At least two types of active sites exist for PCO on TiO_2 and their activities differ by more than an order of magnitude; the more-active sites comprise approximately 30% of the adsorption sites. Water redistributes adsorbed dichloroacetyl chloride and dichloroacetic acid to more-active sites during transient PCO, yet does not change PCO activity or selectivity. Dichloroacetyl chloride oxidizes through parallel pathways, one of which forms dichloroacetic acid as an intermediate. The α -carbon in dichloroacetic acid quickly oxidizes to CO_2 without forming any long-lived intermediates, whereas the β -carbon forms CO_2 and COCl_2 in parallel reactions.

KEY WORDS: dichloroacetyl chloride; dichloroacetic acid; photocatalytic oxidation; TiO_2 .

1. Introduction

Heterogeneous photocatalytic oxidation (PCO) has potential applications for the treatment of waste streams with dilute concentrations of volatile organic compounds because it effectively oxidizes a wide range of both liquid- and vapor-phase organics to environmentally benign compounds at room temperature [1–12]. Photocatalytic oxidation employs UV or near-UV irradiation to oxidize adsorbed organics to CO_2 and H_2O on semiconductor catalysts, such as titanium dioxide (TiO_2). Ultraviolet light excites electrons from the valence to the conduction band of the semiconductor catalyst, leaving holes behind. These electron–hole pairs migrate to the catalyst surface and initiate redox reactions with adsorbed species. Although extensive research has been devoted to the oxidation of aqueous-phase organics, the mechanism may be different for gas-phase reactants [9]. Recent studies have demonstrated that PCO successfully oxidizes many gas-phase organics, but reaction pathways are not fully understood and intermediates are often not identified [1–4,7,9,11,12].

The trichloroethylene (TCE) PCO mechanism merits investigation because TCE is the most common ground contaminate in the United States and is rapidly oxidized by PCO [13]. Some studies reported complete destruction of TCE under certain conditions [14–16], but chlorinated partial oxidation products have been observed in both liquid and vapor phases [14,17,18]. Several researchers [12,14,18–20] reported significant amounts of dichloroacetyl chloride (DCAC) and phos-

gene (COCl_2) from TCE PCO. In steady state experiments with Fourier transform infrared spectroscopy (FTIR), Jacoby *et al.* [19] observed DCAC as a major product of TCE PCO at short residence times and complete destruction of DCAC at longer residence times. This behavior is characteristic of an intermediate. Similarly, Fan and Yates [20] reported that DCAC formed directly from TCE; the maximum DCAC concentration coincided with complete destruction of TCE. Several other studies have also reported DCAC as the major intermediate species of TCE PCO on TiO_2 [12,13,18–22]. The formation of such products is a concern because both DCAC and COCl_2 are considerably more toxic than TCE [23]. Hence, practical implementation of PCO for TCE remediation requires suppressing the formation of these partial oxidation products. This in turn necessitates a more fundamental knowledge of the surface reactions of TCE and its intermediates.

Several PCO studies also identified dichloroacetic acid (DCAA) and other carboxylates during TCE PCO in both aqueous [14] and vapor [20,24] phases. Hwang *et al.* [13] observed surface-bound dichloroacetate on powdered Degussa P-25 TiO_2 after gas-phase TCE PCO using *in situ* solid-state nuclear magnetic resonance methods and attributed dichloroacetate formation to reaction of DCAC with surface hydroxyls (OH). In separate experiments on TiO_2 /PVG, they reported that DCAC reacted with OH to form surface-bound dichloroacetate in the dark; subsequent UV irradiation oxidized dichloroacetate to COCl_2 and CO_2 . The authors concluded that DCAC formed during TCE PCO and underwent immediate hydrolysis to form DCAA, which was a major intermediate of TCE PCO on H_2O -saturated TiO_2 /PVG. Rice and Raftery [23]

* To whom correspondence should be addressed.
E-mail: Darrin_Muggli@und.nodak.edu

also reported DCAC and DCAA formation during gas-phase TCE PCO on optical microfibers coated with Degussa P-25 TiO₂. The authors observed CO₂ and COCl₂ as the major products, with small quantities of DCAA and trichloroacetaldehyde remaining adsorbed after PCO. They also showed that DCAC reacted with OH in the dark.

Although several studies [13,14,20,23,24] identified DCAA as an intermediate of TCE PCO, no effort has been made to investigate DCAA PCO on TiO₂ and to compare it with that of DCAC. In this study, transient PCO and temperature-programed oxidation (TPO) were combined to investigate the PCO reaction pathways of DCAA and DCAC; this study is unique in that it is the first study to use isotope labeling to explore the DCAA PCO mechanism. This study will identify and quantify multiple reaction sites, along with their activities, and explore the role of H₂O during PCO. This study will also show that DCAC initially reacts through DCAA, but oxidizes through another pathway at longer reaction times.

2. Experimental methods

The experimental apparatus used in this study has been described previously [7,10,11,25]. An annular Pyrex reactor allowed for high gas-flow rates and uniform UV irradiation of the catalyst. A thin layer of approximately 30 mg of Degussa P-25 TiO₂ coated the inner surfaces of the photoreactor (with a 1-mm annular gap). A furnace, which consisted of Ni-Cr wire wrapped around a quartz cylinder, encased the reactor and six 8-W UV lamps (Johnlite) surrounded the furnace for PCO experiments. A 0.5-mm chromel–alumel, shielded thermocouple contacted the catalyst film to provide feedback to the temperature controller. A Balzers QMS 200 quadrupole mass spectrometer monitored the reactor effluent directly downstream of the reactor. A 25- μ m i.d. fused silica capillary, which fed directly to the mass spectrometer ionizer, sampled the reactor effluent. The mass spectrometer signals were calibrated by injecting known volumes of each species into the gas flow downstream of the reactor, and signals were corrected for cracking in the mass spectrometer. Integration of the areas under the calibration curves provides a means to convert mass spectrometer signals to reaction rates.

Before each isothermal PCO, the catalyst was heated at a rate of 1 K s⁻¹ to 723 K in 100 sccm flow of 20% O₂ in He (Praxair, UHP) and held at this temperature for 20 min to create a reproducible surface. Two pulses of organic (350 μ mol DCAC/g catalyst each or 340 μ mol ¹³DCAA/g catalyst each) injected upstream of the reactor saturated the catalyst and the carrier gas flushed excess organic from the gas phase before transient PCO began. Although adsorption of ¹³DCAA (Cl₂H¹³CCOOH) was carried out at 100 °C to prevent

condensation of ¹³DCAA on the reactor walls, the catalyst was cooled to room temperature before initiating PCO. Before transient PCO was carried out at room temperature, a shield blocked UV light from the reactor for 10 min as the lights reached a steady output. Removal of the shields exposed the catalyst to UV irradiation and thus initiated transient PCO. After a specified time, terminating UV irradiation stopped PCO and subsequent TPO oxidized the remaining surface species. Temperature-programed oxidation was performed in the same carrier gas flow as PCO by heating the catalyst at 1 K s⁻¹ to 723 K and holding at this temperature until products were no longer detected in the gas phase.

Analysis of rate data consisted of generating plots of reaction rate versus time. In addition, to explore activities of adsorption sites, formation rates of gas-phase products (CO₂ and COCl₂) were normalized by dividing them by the amount of organic that remained adsorbed at each sample point. For a single-step reaction, such as the oxidation of the α -carbon in DCAA, this analysis directly measures the activity of TiO₂ adsorption sites. If all of the adsorption sites were equally active, the normalized rate would be constant for a first-order single-step reaction. For species such as DCAC, the formation of surface intermediates must be considered in the analysis of normalized formation rates.

Owing to safety concerns, COCl₂ calibration was not performed. Instead, a series of experiments determined a relationship between DCAC and COCl₂ signals to base COCl₂ calibration on that of DCAC. First, TPO of DCAC determined DCAC saturation coverage on TiO₂. The saturation coverage of DCAC could be quantified because the mass spectrometer was calibrated for all of the carbon-containing gas-phase TPO products. Next, transient PCO of DCAC with subsequent TPO immediately followed the aforementioned TPO. The calibration factor for COCl₂ was adjusted until the total amount of carbon formed during the transient PCO of DCAC and subsequent TPO equaled the saturation coverage determined from the preceding TPO. Repetition of these experiments yielded COCl₂ calibration factors that differed from each other by less than 1%.

3. Results

3.1. Transient PCO of DCAC

Figure 1(a) shows the gas-phase products from transient PCO of a monolayer of DCAC at room temperature on fresh TiO₂. Upon UV irradiation of the catalyst, adsorbed DCAC quickly oxidized to CO₂ and COCl₂. After reaching initial maxima, CO₂ and COCl₂ formation rates decreased rapidly until termination of UV irradiation stopped further reaction. Adsorbed DCAC initially oxidized to CO₂ approximately twice

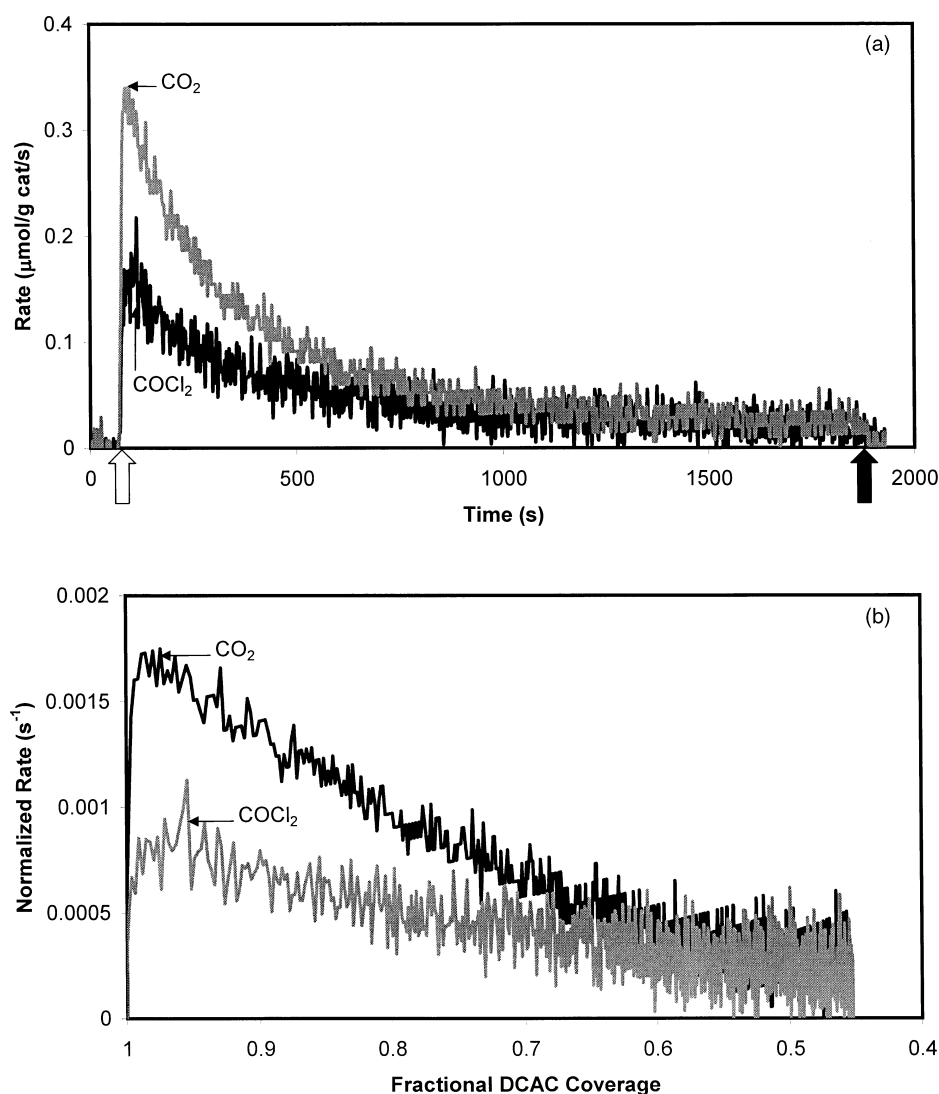


Figure 1. (a) Formation rates and (b) normalized formation rates during transient PCO of a DCAC monolayer on TiO_2 in 20% O_2 at room temperature. The UV lights were turned on at 60 s and turned off at 1800 s.

as fast as to COCl_2 . At longer reaction times, however, CO_2 and COCl_2 form at approximately equal rates. After transient PCO, TPO oxidized the remaining surface species to CO , CO_2 , and HCl . The amounts of CO_2 and COCl_2 formed during transient PCO, combined with those of CO and CO_2 desorbed during subsequent TPO, determined the DCAC monolayer coverage. That is, TPO closed the carbon mass balance by oxidizing the remaining surface species to CO and CO_2 . Dichloroacetyl chloride coverage (approximately $200 \mu\text{mol}$ of DCAC/g catalyst) differed by less than 10% in subsequent experiments.

Figure 1(b) plots normalized rates versus fractional coverage throughout PCO. The normalized CO_2 and COCl_2 formation rates (figure 1(b)) increased to initial maxima and subsequently decreased throughout the experiment. Catalyst activity decreases significantly as PCO oxidizes adsorbed species; at low coverages, the

normalized CO_2 and COCl_2 rates were approximately 10 and 20% of the initial rates respectively.

3.2. Transient PCO of DCAC with pulsed H_2O

Figure 2(a) shows transient PCO of a monolayer of DCAC that was stopped after 300 s, H_2O pulsed in the dark, and PCO resumed after excess H_2O was flushed from the gas phase. For clarity, the dark time shown in figure 2 was shortened; approximately 15 min were required to pulse H_2O , flush the excess from the gas phase, and return UV lights to a steady output. Temperature-programmed oxidation following PCO confirmed that a significant amount of H_2O adsorbed; although water desorption was not complete at the end of TPO, $250 \mu\text{mol}$ of $\text{H}_2\text{O/g}$ catalyst desorbed. In comparison, no H_2O desorbed during TPO after DCAC

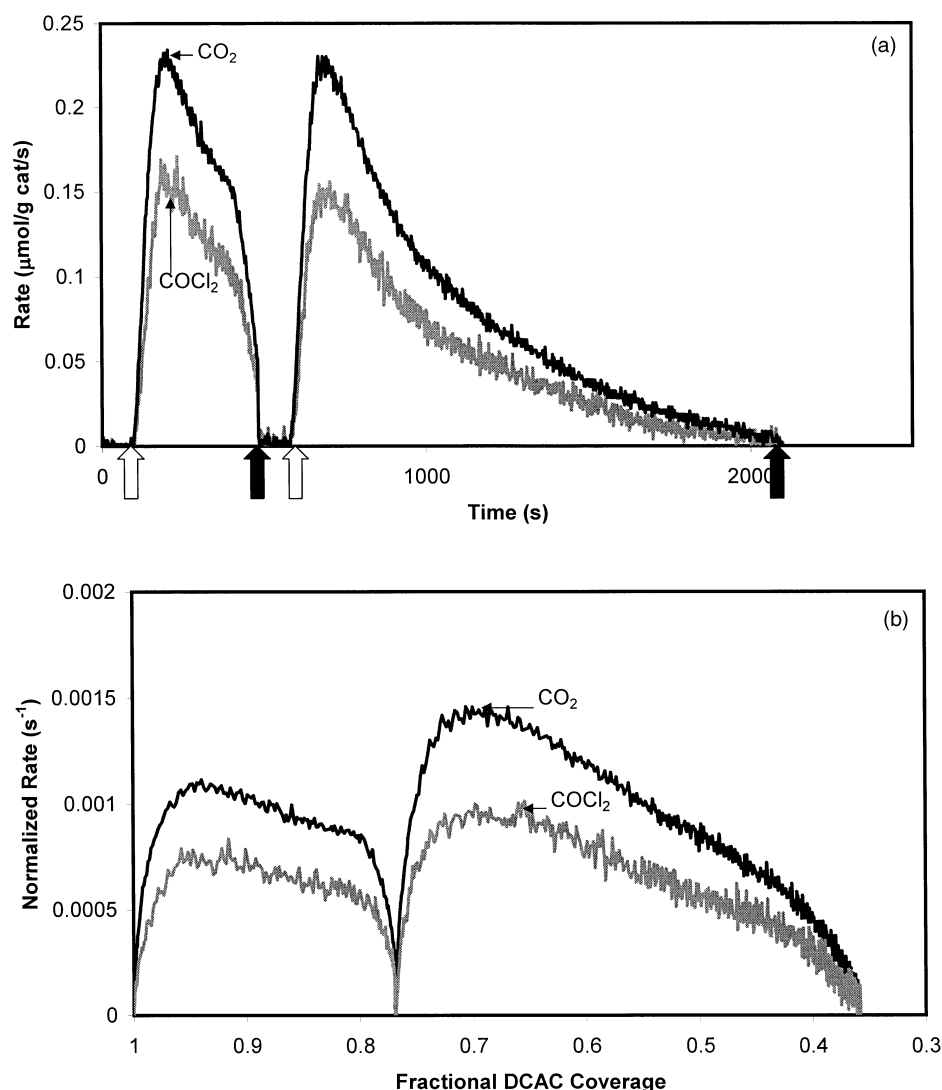


Figure 2. (a) Formation rate and (b) normalized formation rates during transient PCO of DCAC. The lights were turned off (black arrows) and on (white arrows) during the experiment. During the dark period, H_2O was injected and flushed from the gas phase before UV irradiation reinitiated PCO.

PCO on fresh TiO_2 . When PCO resumed after H_2O injection, CO_2 and COCl_2 formation rates were approximately 50% greater than that immediately before UV termination and attained the same maxima as that attained initially; H_2O apparently redistributed DCAC to more-active sites vacated by the 300-s PCO. The initial maximum rates (figure 2(a)) are lower than those seen in figure 1(a) because the quartz furnace darkened with use, thereby decreasing UV intensity. However, the initial maximum rates were different by less than 15% in repeat experiments. The selectivity was the same before and after H_2O injection and, as shown in figure 1, DCAC PCO selectivity to CO_2 decreased at longer reaction times. Repeat experiments showed that the initial selectivity to CO_2 was 2 ± 0.6 (95% confidence limits).

After H_2O injection, CO_2 and COCl_2 normalized formation rates (figure 2(b)) were approximately 80% greater than that immediately before UV termination and approximately 25% greater than the initial maxima

from the 300-s PCO. A control experiment verified that mass transfer limitations did not cause the increased rates after H_2O pulse in the dark; the lights were shut off for the same time required to inject and flush H_2O from the gas phase (15 min). If diffusion of O_2 to the surface limited PCO, increased rates would be expected after the dark time. Similarly, increases in rates after the dark time would be expected if surface diffusion of DCAC or active oxygen species limited PCO. After reinitiating PCO, however, rates were the same as that immediately before UV termination. That is, neither gas-phase nor surface-diffusion limitations caused the observed rate increases after the dark time.

3.3. Transient PCO of $^{13}\text{DCAA}$

Initially, transient PCO quickly oxidized a monolayer of $^{13}\text{DCAA}$ ($\text{Cl}_2\text{H}^{13}\text{CCOOH}$, figure 3(a)) to $^{12}\text{CO}_2$,

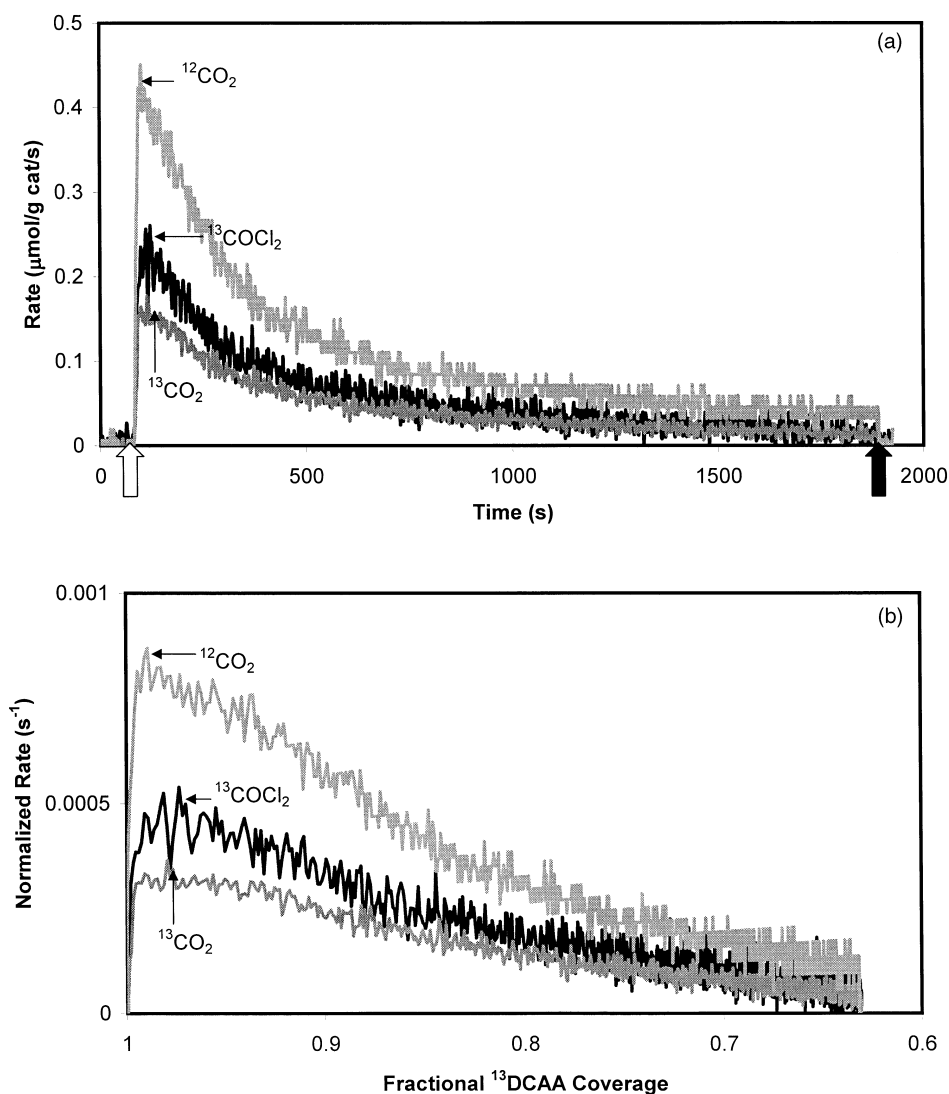


Figure 3. (a) Formation rates and (b) normalized formation rates during transient PCO of a $^{13}\text{DCAA}$ monolayer on TiO_2 in 20% O_2 at room temperature. The UV lights were turned on at 60 s and turned off at 1800 s.

$^{13}\text{CO}_2$, and $^{13}\text{COCl}_2$. No gas-phase $^{12}\text{COCl}_2$ was observed in the reactor effluent, indicating that phosgene only forms from the β -carbon of DCAA. Subsequently, $^{12}\text{CO}_2$, $^{13}\text{CO}_2$, and $^{13}\text{COCl}_2$ formation rates decreased after reaching initial maxima until termination of UV irradiation stopped further reaction. Adsorbed $^{13}\text{DCAA}$ oxidized to CO_2 ($^{12}\text{CO}_2 + ^{13}\text{CO}_2$) approximately twice as fast as it formed COCl_2 . Selectivity to CO_2 remained constant throughout DCAA PCO, whereas that of DCAC PCO (figure 1) decreased at longer reaction times. The total CO_2 and COCl_2 rates, as well as coverage, from $^{13}\text{DCAA}$ PCO were the same as those from $^{12}\text{DCAA}$ PCO, which indicates that all gas-phase species were correctly identified.

Similar to DCAC PCO, the normalized formation rates (figure 3(b)) during DCAA PCO reached initial maxima and subsequently decreased throughout PCO. If all of the adsorption sites were equally active, the normalized rate would be constant for a first-order

single-step reaction. Although a second-order reaction could produce the decreasing normalized rates seen in figure 3(b), the rate normalized by the square of coverage (not shown) also decreased throughout PCO. For a second-order reaction in which all adsorption sites are equally active, the rate normalized by the square of coverage would be constant throughout PCO. Alternatively, the decrease in normalized rate (figure 3(b)) suggests more than one type of active site for PCO [26,27].

3.4. Transient PCO of $^{13}\text{DCAA}$ with pulsed H_2O

As previously described for DCAC, H_2O was injected into the reactor in the dark and flushed from the gas phase after 300 s of $^{13}\text{DCAA}$ PCO (figure 4) before UV irradiation reinitiated PCO. Temperature-programmed oxidation after $^{13}\text{DCAA}$ PCO with pulsed H_2O con-

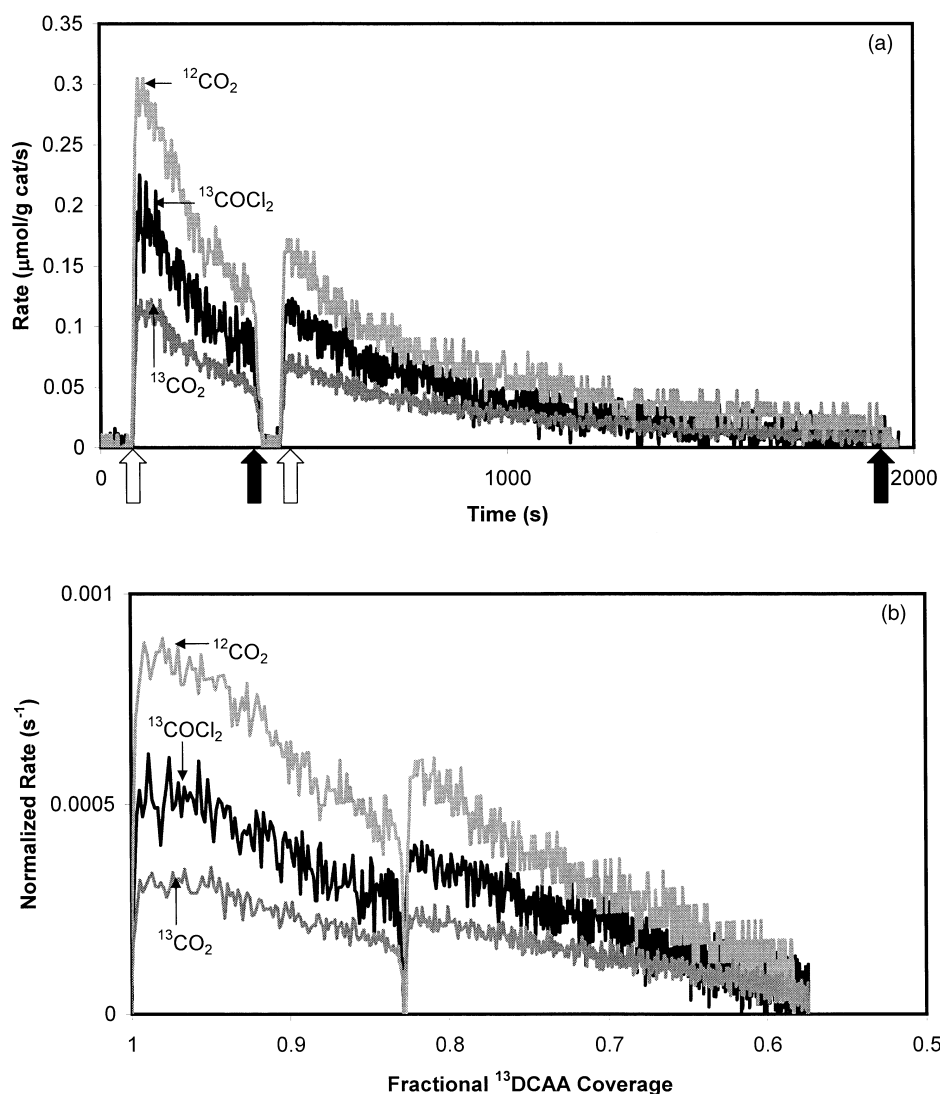


Figure 4. (a) Formation rate and (b) normalized formation rates during transient PCO of $^{13}\text{DCAA}$. The lights were turned off (black arrows) and on (white arrows) during the experiment. During the dark period, H_2O was injected and flushed from the gas phase before UV irradiation reinitiated PCO.

firmed the presence of H_2O on the catalyst surface; although water desorption was not complete at the end of TPO, $150 \mu\text{mol}$ of $\text{H}_2\text{O/g}$ catalyst desorbed. Similar to DCAC, H_2O desorption was not detected during TPO after $^{13}\text{DCAA}$ PCO on fresh TiO_2 ; hydrogen in DCAA desorbed as HCl during TPO.

Upon UV irradiation of the catalyst, adsorbed $^{13}\text{DCAA}$ quickly oxidized to $^{12}\text{CO}_2$, $^{13}\text{CO}_2$, and $^{13}\text{COCl}_2$. Again, no gas-phase $^{12}\text{COCl}_2$ formed. Subsequently, all of the product formation rates decreased after reaching initial maxima. After H_2O injection in the dark, $^{12}\text{CO}_2$, $^{13}\text{CO}_2$, and $^{13}\text{COCl}_2$ formation rate maxima were approximately 40% greater than that immediately before UV termination and approximately 60% of initial maxima from the 300-s PCO. Similar to DCAC, H_2O apparently redistributed $^{13}\text{DCAA}$ to more-active sites vacated by 300 s of PCO. In contrast to DCAC PCO, however, $^{13}\text{DCAA}$ PCO formation

rates after H_2O injection did not attain the same maxima as that attained initially. A two-site model, which is discussed later, predicted that H_2O displaced only 5% of a $^{13}\text{DCAA}$ monolayer. Water did not significantly change $^{13}\text{DCAA}$ coverage, which indicates that nearly all the displaced $^{13}\text{DCAA}$ readsorbed. Similar to DCAC PCO (figure 2), injecting H_2O did not change $^{13}\text{DCAA}$ PCO selectivity.

4. Discussion

4.1. Active sites

Plots of normalized rate versus fractional coverage (figures 1(b) and 3(b)) provide information about catalyst activity. For a first-order reaction in which all adsorption sites are equally active, the normalized rate would be constant throughout PCO. However, the

normalized rates from both DCAC (figure 1(b)) and $^{13}\text{DCAA}$ PCO (figure 3(b)) quickly reached initial maxima and subsequently decreased throughout PCO. Similar to formic acid PCO [27], figures 1 and 3 are consistent with two types of active sites. At low coverages, the normalized rates were nearly an *order of magnitude* lower than the initial rates because nearly all of the species adsorbed on more-active sites had reacted and, primarily, species adsorbed on less-active sites remained.

As shown previously [27], the formation rate of gas-phase CO_2 monitors the surface reaction rate because CO_2 does not adsorb significantly on TiO_2 at room temperature. That is, evolution of gas-phase CO_2 is not diffusion-limited and directly measures the surface PCO rate. Furthermore, the $^{12}\text{CO}_2$ formation rate directly measures the $^{13}\text{DCAA}$ PCO rate because the α -carbon of DCAA is expected to oxidize in a single step, in agreement with previous observations of other carboxylates [11,27,28]. Therefore, the $^{12}\text{CO}_2$ decay curve (figure 3) was fit to a two-site model of $^{13}\text{DCAA}$ PCO to quantify more- and less-active sites with their respective activities. Similar to previous studies [18,27,29], the two-site model assumes constant oxygen concentration and therefore first-order surface reactions.

Because mass balances determine the initial $^{13}\text{DCAA}$ coverage, the model contains three adjustable parameters: site 1 activity, site 2 activity, and the ratio of organic coverage on sites 1 and 2. Figure 5 illustrates the two-site model fit to the $^{12}\text{CO}_2$ decay curve (figure 3(a)). The value determined for the $^{13}\text{DCAA}$ model for site 1 activity ($k_1 = 4 \times 10^{-3} \text{ s}^{-1}$) was approximately 20 times that of site 2 ($k_2 = 2 \times 10^{-4} \text{ s}^{-1}$). Approximately 30% of $^{13}\text{DCAA}$ adsorbed on the surface reacted on more-active sites. Similarly, Muggli and Backes [27] reported that approximately one-fourth of the sites were highly

active for formic acid PCO on TiO_2 and that site 1 was approximately 20 times more active than site 2.

Employing the same method as this study, Muggli and Backes [27] reported that H_2O , which formed during formic acid PCO on TiO_2 , easily removed a fraction of adsorbed formic acid. They also reported that H_2O injections during formic acid PCO displaced formic acid to more-active sites. The authors determined that two active sites existed for formic acid PCO on TiO_2 and that H_2O redistributed species on the surface. Utilizing the same experimental apparatus as this study, Muggli and Backes [27] also showed that the decreasing normalized rate was not due to experimental artifacts such as nonuniform UV irradiation, surface diffusion of organic or oxygen species, desorption or gas-phase diffusion of CO_2 , or deactivation due to accumulation of H_2O during PCO.

Although DCAA quickly oxidized to CO_2 and COCl_2 upon UV irradiation as shown in figures 3 and 4, other studies [13,23,24] reported that dichloroacetate photooxidized slowly and observed that dichloroacetate adsorbed on the catalyst surface after TCE PCO. The existence of two active sites would explain the apparent discrepancy between this study and previous steady state experiments [13,23,24]. In steady state studies, PCO rates simultaneously measure the activity of all sites because more-active sites are continually replenished by gas-phase species. After steady state PCO, dichloroacetate presumably adsorbed on less-active sites is expected to remain on the surface because it reacts slowly and is more strongly bound than other species, such as TCE and DCAC. In transient studies, however, the *initial* PCO rate primarily measures the activity of more-active sites. That is, chlorinated organics react readily on more-active sites and produce high *initial* reaction rates in transient studies.

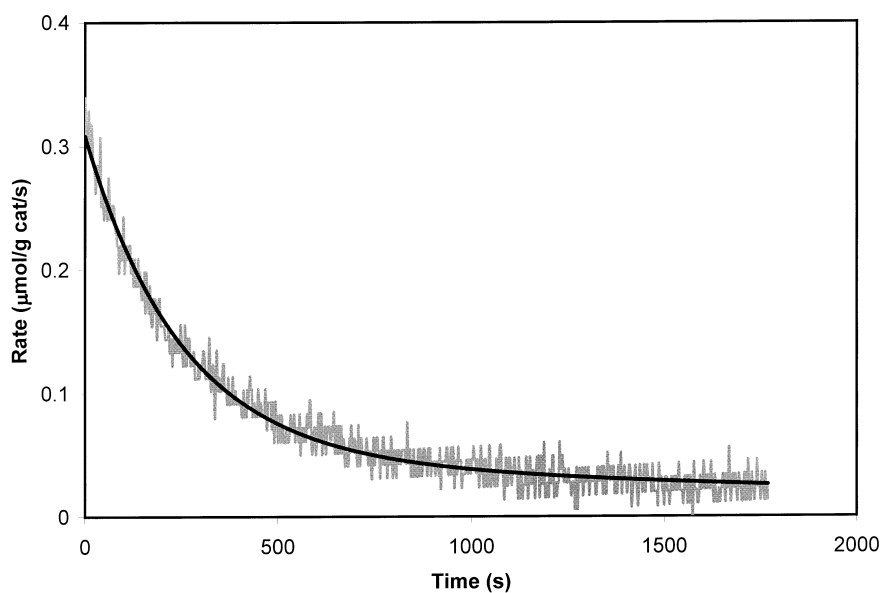


Figure 5. Decay curve for $^{12}\text{CO}_2$ formation from $^{13}\text{DCAA}$ PCO with a two-site model fit.

4.2. Effect of H₂O

Water does not appear to change activity or selectivity during DCAA and DCAC PCO. In a series of coadsorption experiments (not shown), H₂O was introduced into the reactor system in the dark after organic adsorption. During subsequent PCO of coadsorbed DCAC and H₂O, H₂O did not increase PCO rates or change selectivity. A similar experiment that coadsorbed H₂O and ¹³DCAA also showed that H₂O did not change catalyst activity or selectivity. Seemingly in contrast to these experiments, figures 2 and 4 show that injecting H₂O after 300 s of PCO increased PCO rates. The existence of two active sites resolves the seeming discrepancy between the coadsorption experiments and figures 2 and 4. The 300-s PCO preferentially depleted more-active sites, which oxidize adsorbed organic quickly, and species remaining adsorbed after UV termination primarily occupied less-active sites. Water injection after 300 s of PCO displaced adsorbed DCAC, redistributing it on the surface, and effectively increased DCAC coverage on more-active sites. Hence, figures 2 and 4 are consistent with the coadsorption experiments; H₂O in and of itself does not increase the PCO rate. Injecting H₂O increased DCAC PCO rates more than those of DCAA presumably because H₂O displaces DCAC more readily than DCAA. The two-site model predicted that injecting H₂O replenished approximately 25% of the more-active sites depleted by the initial 300-s PCO. Water evidently completely replenished DCAC consumed on the more-active sites because the maximum rates after H₂O injection (figure 2(a)) were greater than the initial maxima. This suggests that DCAA adsorbed on TiO₂ more strongly than DCAC.

As suggested by previous studies [12,13,18–22], in addition to redistributing DCAC to more-active sites, injecting H₂O in the dark could also replenish surface OH groups that may have been consumed by the 300-s PCO. Rice and Raftery [23] reported that DCAC quickly reacts with surface hydroxyls in the dark to form DCAA. Hwang *et al.* [13] observed dichloroacetate as a surface species during TCE PCO under hydrated conditions using ¹³C MAS NMR and also attributed DCAA formation to a dark reaction between DCAC and surface hydroxyls. They observed significant DCAC formation in the early stages of TCE PCO, while DCAA formation occurred later with a concomitant decrease in DCAC.

To determine if the increase in PCO rate upon H₂O injection was due to resupplying surface hydroxyls rather than redistributing adsorbed species to more-active sites, another set of experiments (not shown) replicated the procedure used in figures 2 and 4, except that the catalyst was heated to 373 K and subsequently cooled to room temperature in the dark, instead of injecting H₂O. These experiments produced results nearly identical to those of figures 2 and 4, indicating

that the effect of heating was the same as injecting H₂O. That is, heating also redistributed adsorbed species on the surface. In agreement with these results, Fan and Yates [20], using oxygen-labeled H₂O, reported no incorporation of the oxygen label into any gas-phase products of TCE PCO; the products contained only oxygen-18 from gas-phase O₂. The authors concluded that electronically activated, chemisorbed O₂ on TiO₂ photooxidizes TCE and that gas-phase mechanisms based on hydroxyl radicals were not valid, although they also suggested that DCAA formed from DCAC hydrolysis because H₂O decreased DCAC yields and increased CO₂ yields during TCE PCO.

At low humidity levels, Jacoby *et al.* [19] reported that in steady state experiments DCAC PCO selectivity to CO₂ was two, in agreement with this study. However, they observed that selectivity to CO₂ increased to four at humidity levels greater than 1000 mtorr. Jacoby *et al.* [19] attributed the selectivity change with increased humidity to a parallel reaction pathway for DCAC PCO. Although they concluded that H₂O decreased the COCl₂ formation rate during DCAC PCO, the results of this study show that H₂O did not inhibit COCl₂ formation.

In the studies [12,13,18–22] that reported increased selectivity to CO₂ at elevated humidity levels, PCO was performed in the presence of gas-phase organics, whereas in this study gas-phase organics were flushed from the reactor before PCO was initiated. Therefore, weakly adsorbed species that were present during steady state studies would be absent in this transient study. Because weakly adsorbed species would be readily displaced by H₂O, increased humidity levels would change the coverage of these weakly adsorbed species and thus would change selectivity if these species react differently than those that are strongly adsorbed. Adding H₂O during transient PCO, however, had little effect on selectivity, presumably because weakly adsorbed species have already been removed. Thus, the absence of gas-phase species would explain the apparent discrepancy between the results of this study and those published previously [12,13,18–22]. This demonstrates the utility of comparing steady state PCO to transient reaction studies, which measure the PCO behavior of species that remain on the surface in the absence of gas-phase organics.

4.3. Photocatalytic oxidation reaction pathways

Figures 1(a) and 3(a) show that initially, both DCAA and DCAC oxidize to CO₂ twice as fast as they form COCl₂. At longer reaction times, DCAC, however, formed CO₂ and COCl₂ at the same rate, whereas DCAA continued to produce CO₂ at twice the rate of COCl₂. Because CO₂ formation primarily measures the activity of more-active sites at early reaction times, the

more-active sites exhibit a selectivity of two. Similarly, the CO_2 formation rate mainly reflects the activity of less-active sites at longer reaction times when organic adsorbed on more-active sites has primarily been consumed. That is, less-active sites for DCAC PCO apparently yield a selectivity of one. In contrast, less-active and more-active sites for DCAA PCO both exhibit a selectivity of two. Although DCAC PCO initially exhibits the same selectivity to CO_2 as that of DCAA, the decrease in DCAC PCO selectivity at longer reaction times suggests that DCAC reacts through a parallel pathway that initially proceeds through DCAA.

Temperature-programmed oxidation spectra (not shown) taken after DCAC and DCAA PCO were nearly identical. This indicates that DCAC and DCAA form the same surface species during PCO and further suggests that DCAA is a primary intermediate of DCAC PCO. As previously discussed, researchers [12,13,18] have also suggested that DCAC forms DCAA during gas-phase PCO, in agreement with this study; Kenneke *et al.* [14] also observed DCAA formation from aqueous-phase TCE PCO. Although DCAC reacts through DCAA initially and through another pathway at longer reaction times, the similarities in TPO spectra after DCAC and DCAA PCO indicate that the surface species from this alternate pathway are identical or similar to those from DCAA PCO.

The results of this study also reveal information about the reaction pathway of DCAA. Chemseddine and Boehm [14] attributed the evolution of CO_2 from aqueous DCAA PCO to the carboxyl group alone. Figures 3 and 4, however, clearly show that CO_2 evolved from both carbons, whereas COCl_2 only formed from the β -carbon of DCAA. Because the formation rates of $^{13}\text{CO}_2$ and $^{13}\text{COCl}_2$ reach maxima simultaneously, evolution of $^{13}\text{CO}_2$ from $^{13}\text{COCl}_2$ is unlikely. In agreement, Hwang *et al.* [13] reported that COCl_2 formed during TCE PCO did not oxidize further under continued UV irradiation. That is, only a small amount, if any, of COCl_2 forms CO_2 in the timescale of the experiments in this study. If $^{13}\text{COCl}_2$ oxidized to $^{13}\text{CO}_2$, the maximum $^{13}\text{CO}_2$ formation rate would occur later than that of $^{13}\text{COCl}_2$. Furthermore, selectivity to COCl_2 would be expected to decrease throughout the experiment if $^{13}\text{COCl}_2$ formed $^{13}\text{CO}_2$, whereas that of a parallel reaction would be expected to be constant throughout the experiment, assuming the same order for both reactions. Figures 2 and 4 show that selectivity is constant and suggest a parallel reaction pathway for the β -carbon of DCAA.

5. Conclusions

During PCO on TiO_2 , both DCAC and DCAA oxidize quickly to form CO_2 and COCl_2 . Approximately

30% of the adsorption sites are highly active for PCO. Although H_2O has little impact on DCAC and DCAA PCO activity and selectivity, it displaces both species. Initially, DCAC appears to react through a DCAA intermediate, but oxidizes through another pathway at longer reaction times. Dichloroacetic acid PCO forms COCl_2 from the β -carbon of DCAA, whereas CO_2 forms from both carbons.

Acknowledgments

This material is based upon work supported by the National Science Foundation under Grant No. #0132289. The Donors of the Petroleum Research Fund, administered by the American Chemical Society, and the North Dakota Experimental Program to Stimulate Competitive Research (ND EPSCoR) are acknowledged for support of this research. Adrienne C. Lukaski gratefully acknowledges the Environmental Protection Agency Students Engaged in Environmental Research Program (EPA STEER) and the ND EPSCoR Advanced Undergraduate Research Award (AURA) Program.

References

- [1] M.-L. Sauer and D.-F. Ollis, *J. Catal.* 149 (1994) 81.
- [2] M.R. Nimlos, E.J. Wolfrum, M.L. Brewer, J.A. Fennell and G. Bintner, *Environ. Sci. Technol.* 30 (1996) 3102.
- [3] A.V. Vorontsov, G.B. Barannik, O.I. Snegurenko, E.N. Savinov and V.N. Parmon, *Kinet. Catal.* 38 (1997) 84.
- [4] N.R. Blake and G.L. Griffin, *J. Phys. Chem.* 92 (1988) 5697.
- [5] J.C. Kennedy and A.K. Datye, *J. Catal.* 179 (1998) 375.
- [6] J.L. Falconer and K.A. Magrini-Bair, *J. Catal.* 179 (1998) 171.
- [7] D.S. Muggli and J.L. Falconer, *J. Catal.* 175 (1998) 213.
- [8] D.S. Muggli and J.L. Falconer, *J. Catal.* 191 (2000) 318.
- [9] D.S. Muggli, J.T. McCue and J.L. Falconer, *J. Catal.* 173 (1998) 470.
- [10] D.S. Muggli, K.H. Lowery and J.L. Falconer, *J. Catal.* 180 (1998) 111.
- [11] D.S. Muggli, S.A. Larson and J.L. Falconer, *J. Phys. Chem.* 100 (1996) 15886.
- [12] W.A. Jacoby, D.M. Blake, R.D. Noble and C.A. Koval, *J. Catal.* 157 (1995) 87.
- [13] S.J. Hwang, C. Petucci and D. Raftery, *J. Am. Chem. Soc.* 120 (1998) 4388.
- [14] M.A.Y.-N. Anderson and S. Cervera-March, *Photocatal. Purif. Treatment Water Air* (1993) 405.
- [15] S. Yamazaki Nishida, S. Cervera-March, K.J. Nagano, M.A. Anderson and K. Hori, *J. Phys. Chem.* 99 (1995) 15814.
- [16] W.-A. Zeltner, C.-G. Hill Jr. and M.-A. Anderson, *CHEMTECH* 23 (1993) 21.
- [17] W.-H. Glaze, J.-F. Kenneke and J.-L. Ferry, *Environ. Sci. Technol.* 27 (1993) 177.
- [18] M.R. Nimlos, W.A. Jacoby and D.M. Blake, *Environ. Sci. Technol.* 27 (1993) 732.
- [19] W.A. Jacoby, M.R. Nimlos and D.M. Blake, *Environ. Sci. Technol.* 28 (1994) 1661.
- [20] J.F. Fan and J.T. Yates, *J. Am. Chem. Soc.* 118 (1996) 4686.
- [21] J.S. Kim, K. Itoh and M. Murabayashi, *Denki Kagaku* 65 (1997) 966.

- [22] P.B. Amama, K. Itoh and M. Murabayashi, J. Mol. Catal., A: Chem. 176 (2001) 165.
- [23] C.V. Rice and D. Raftery, Chem. Commun. (1999) 895.
- [24] J.S. Kim, K. Itoh and M. Murabayashi, Chemosphere 36 (1998) 483.
- [25] S.A. Larson, J.A. Widegren and J.L. Falconer, J. Catal. 157 (1995) 611.
- [26] D.S. Muggli and L.F. Ding, Appl. Catal., B: Environ. 32 (2001) 181.
- [27] D.S. Muggli and M.J. Backes, J. Catal. 209 (2002) 105.
- [28] D.S. Muggli and J.L. Falconer, J. Catal. 187 (1999) 230.
- [29] H. Liu, S.A. Cheng, J.Q. Zhang, C.N. Cao and W.C. Jiang, Chemosphere 35 (1997) 2881.